ACS OMEGA

Open Access

http://pubs.acs.org/journal/acsodf

Article

Evaluation, Reduction, and Validation of a New Skeletal Mechanism for the Cofiring of NH_3 and CH_4

Yuhang Li, Zhonghua Jin, Zhichao Wang, Houzhang Tan,* Zixiu Jia, Baochong Cui, Shangkun Zhou, and Faqi Bai

Cite This: *ACS Omega* 2023, 8, 47113−47122

Read Online

ACCESS | Metrics & More | Article Recommendations | Supporting Information

ABSTRACT: The evaluation and reduction of kinetic models for the cofiring of NH_3 and CH_4 can help to guide the application of NH_3 and CH_4 in industrial equipment. In this work, eight detailed kinetic models on the cofiring of NH_3 and CH_4 and 15 detailed kinetic models on the NH_3 combustion are collected and evaluated based on error function and experiment measurement, and the detailed mechanism of 169 species and 1268 elementary reactions with the best overall performance was determined. By using two mechanism reduction methods of directed relation graph with error propagation (DRGEP) and DRGEP with sensitivity analysis (DRGEPSA), the skeletal mechanism of 45 species and 344 elementary reactions is achieved within the temperatures of 1000−2000 K, pressures of 1−60 atm, and equivalence ratios of 0.5−2.0. The skeletal mechanism is comprehensively validated and achieves good consistency with the detailed mechanism in predicting the laminar burning velocity, species concentration, and ignition delay time. The maximum relative error between the skeletal mechanism and the detailed mechanism is less than 13%.

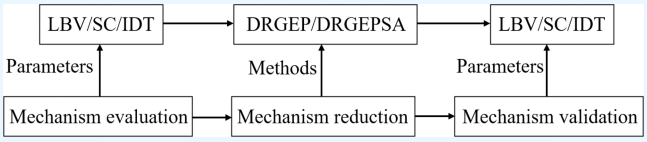

1. INTRODUCTION

To achieve carbon peaking and carbon neutrality as soon as possible, many governments are making efforts. The realization of the two goals depends on the development and application of alternative fuels and their combustion technologies.[1] Hydrogen (H_2) is a typical carbon-neutral fuel, and its substitution for fossil fuels can significantly reduce carbon dioxide (CO_2) emissions. However, the liquefaction requirements for H_2 are relatively harsh (70 MPa at ambient temperature or 20 K at ambient pressure), limiting its large-scale application.[2] Recently, ammonia (NH_3) has attracted widespread attention as the carrier of H_2 due to its relatively mild liquefaction conditions (1.03 MPa at ambient temperature or 239.6 K at ambient pressure).[3] In areas with surplus renewable energy, renewable energy will be directly converted to H_2 through water electrolysis technology. In areas with poor renewable energy, H_2 can be synthesized into NH_3 through the thermochemistry method (Haber−Bosch process). The direct utilization of NH_3 can also reduce the energy loss without conversion to H_2.[4]

However, combustion of neat ammonia still has drawbacks such as low flame speed,[5] sensitivity to nitrogen oxide formation,[6] and difficulty in controlling ammonia slip.[7] Blending with highly reactive fuels such as CH_4,[8,9] H_2,[10] syngas,[11,12] and methanol[13,14] can significantly improve the flame speed of ammonia combustion and control ammonia slip. In addition, blending with fossil fuels such as CH_4[15] and coal[16,17] can also reduce CO_2 emissions.

Numerical simulation can guide the cofiring of NH_3 and CH_4 in industrial equipment such as gas boilers, gas turbines, and internal combustion engines. A kinetic model is essential to simulate the ignition and combustion processes of NH_3/CH_4 cofiring in numerical simulation. However, the recently developed detailed kinetic models of NH_3/CH_4 suffer from the poor flexibility of combustion parameters. For example, the Okafor kinetic model focuses on predicting laminar flame velocity, and there are obvious flaws in predicting nitrogen oxide formation.[18] The Glarborg kinetic model focuses on the formation of NO, and there is a certain overestimation in predicting the NH_3 reactivity and laminar flame velocity.[19] The Dai kinetic model has improved its prediction in ignition delay time of NH_3/CH_4 based on the Glarborg kinetic model by updating the rate constants of $NH_2 + NH_2(+M) = N_2H_4(+M)$,[20] but its prediction in NH_3 reactivity and laminar flame velocity is not significantly different from that of the Glarborg kinetic model. The Arunthanayothin kinetic model has significant biases in predicting laminar flame velocity and N_2O formation.[21] The Zhou kinetic model slightly overestimated the laminar flame velocity.[22,23] Overall, although numerous chemical reaction kinetic models for the cofiring of NH_3/CH_4 have been developed, the comprehensive performance of these kinetic models in predicting laminar burning

Received: September 16, 2023
Revised: November 5, 2023
Accepted: November 14, 2023
Published: November 27, 2023

Table 1. Detailed Mechanism Summary

no.	mechanism	year	species	reactions	description	references
1	GRI 3.0	1999	53	325	NH_3/CH_4 combustion	31
2	Tian	2009	85	703	NH_3/CH_4 combustion	32
3	San Diego	2016−2018	68	311	NH_3 ignition	33
4	Okafor	2018	60	357	NH_3/CH_4 combustion	18
5	Glarborg	2018	151	1397	NOx formation	19
6	Dai	2020	151	1397	NH_3/CH_4 ignition	20
7	Arunthanayothin (Aru)	2021	156	2437	NH_3/CH_4 combustion	21
8	Zhou	2023	169	1268	NH_3/CH_4 combustion	23
9	Song	2016	34	204	NH_3 combustion	35
10	Stagni	2020	31	203	NH_3 combustion	5
11	Han	2020	35	177	NH_3/syngas combustion	36
12	Mei	2020	39	255	NH_3/syngas combustion	12
13	Shrestha	2021	125	1099	NH_3/H_2 combustion	37
14	Zhang	2021	38	263	NH_3/H_2 combustion	38
15	Tang	2022	35	211	NH_3 combustion	39

velocity (LBV), species concentration (SC), and ignition delay time (IDT) has not been thoroughly evaluated.

Due to the limitations of computer costs, detailed kinetic models are difficult to apply in the simulation of combustion processes. The detailed mechanism usually needs to be reduced to a skeletal mechanism. At present, the main mechanism reduction methods can be classified into several categories based on the basic algorithm, such as graph-based,[24,25] sensitivity analysis,[26] time scale-based,[27] species lumping,[28] and reaction-based.[29] Graph-based and sensitivity analysis methods have been widely used and has achieved good performances in mechanism reduction.[30] Therefore, the two methods are also adopted in this work.

In summary, the purpose of this work is (1) to evaluate the developed kinetic models for the cofiring of NH_3/CH_4 to obtain the optimal kinetic model and (2) to reduce the optimal kinetic model using two mechanism reduction methods of directed relation graph with error propagation (DRGEP) and DRGEP with sensitivity analysis (DRGEPSA).

2. RESEARCH METHODS

2.1. Detailed Mechanisms. Table 1 shows the developed detailed kinetic models. Nos. 1−8 can be used to simulate the cofiring of NH_3/CH_4, and nos. 1−15 can be used to simulate the combustion of NH_3. The GRI 3.0 kinetic model has been widely used to simulate the ignition, laminar flame velocity, and NO emissions of natural gas in air.[31] With the recent deepening of research on NH_3 combustion, this mechanism has shown significant limitations in N chemistry. The Tian kinetic model has been developed primarily to simulate the formation of nitrogen oxides under low-pressure conditions.[32] The San Diego model has been developed primarily to simulate the ignition process of N-containing species.[33] The Okafor kinetic model was created on the basis of the GRI 3.0 kinetic model and Tian kinetic model, but this model only verified the laminar flame velocity measured by them; therefore, the prediction performance on other combustion parameters is still unknown.[18] The Glarborg model is recently developed to simulate the formation of nitrogen oxides. Compared with previous models, this model has made significant progress in predicting species concentrations and has been widely used.[19] The Dai model modified the elementary reaction of $NH_2 + NH_2(+M) = N_2H_4(+M)$ based on the Glarborg model, thus improving the prediction on ignition characteristics of NH_3/CH_4.[20] The Arunthanayothin model[21] was developed based on the Stagni model[5] and Aramco 3.0 model.[34] The Zhou model[23] is a detailed kinetic model recently developed, which has been validated by laminar flame velocity and species concentration measurement in detail. Additionally, to compare the performance of ammonia chemistry, another seven models are also selected for comparison. In the following, the 15 kinetic models are simplified as GRI 3.0,[31] Tian,[32] San Diego,[33] Okafor,[18] Glarborg,[19] Dai,[20] Aru,[21] Zhou,[23] Song,[35] Stagni,[5] Han,[36] Mei,[12] Shrestha,[37] Zhang,[38] and Tang[39] mechanisms.

2.2. Experiment Setup and Simulation Methods. Table 2 shows the combustion parameters, experimental setup, and simulation methods in this work. The simulation of laminar burning velocity (LBV), species concentration (SC), and ignition delay time (IDT) is performed in the premixed laminar flame speed, perfect stirred reactor, plug flow reactor, and homogeneous modules of Chemkin-Pro, respectively.

Table 2. Experiment Setup and Simulation Methods

combustion parameters	experiment method	simulation method
laminar burning velocity (LBV)	pherical diffusion flame (SDF)	premixed laminar flame speed
	heat flux method (HFM)	
species concentration (SC)	jet-stirred reactor (JSR)	perfect stirred reactor
	flow reactor (FR)	plug flow reactor
ignition delay time (IDT)	shock tube (ST)	homogeneous
	rapid compression machine (RCM)	

2.3. Summary of Typical Combustion Experiments. Table 3 shows the typical combustion experiments for the cofiring of NH_3 and CH_4. It includes eight data sets with a total of 707 data points, including 192 laminar flame velocity experimental points, 332 species concentration experimental points, and 183 ignition delay time experimental points for mechanism evaluation.

Table 4 shows the typical combustion experiments of NH_3. It includes 11 data sets with a total of 401 data points, including 55 laminar flame velocity experimental points, 174 species concentration experimental points, and 172 ignition delay time experimental points for mechanism evaluation.

https://doi.org/10.1021/acsomega.3c07094
ACS Omega 2023, 8, 47113−47122

Table 3. Summary of Typical Combustion Experiments of NH_3/CH_4

combustion parameters	method	P/atm	T/K	ϕ	data number	references
LBV	SDF	1	298−423	0.7−1.4	33	22
	SDF	1	298	0.7−1.5	64	8
	SDF	1−5	298	0.7−1.5	95	40
SC	JSR	1.25	1000−1200	0.5−2.0	83	21
	FR	1.25	1073−2073	1.0	79	
	JSR	1	950−1400	0.5−2.0	170	23
IDT	RCM	30−60	900−1100	0.5−2.0	45	20
	RCM	20−40	900−1100	0.5−2.0	138	41

Table 4. Summary of Typical Combustion Experiments of NH_3

combustion parameters	method	P/atm	T/K	ϕ	data number	references
LBV	SDF	1−3	473	0.8−1.4	14	10
	SDF	1	373	0.8−1.3	24	42
	SDF	1	298−423	0.8−1.3	17	22
SC	FR	1.25	1373−1973	0.375	50	5
	JSR	1.05	1000−1200	0.01−0.02	19	5
	JSR	1	1150−1280	0.25−1.0	22	38
	JSR	1	1200−1400	0.5−2.0	83	23
IDT	ST	16−42	1183−1581	0.5−2.0	31	43
	ST	1−30	1564−2489	0.5	79	44
	ST	1−10	1440−1900	1.0	18	45
	RCM	60−70	1060−1200	0.5−3.0	44	46

2.4. Quantitative Error Evaluation Method. To quantitatively obtain the performance of different mechanisms on different combustion parameters, we used the following error evaluation function to evaluate the overall deviation between 1108 experimental data points and the simulated values of 15 mechanisms.

$$E_i = \frac{1}{N_i}\sum_{j=1}^{N_i}\left(\left|\frac{Y_{ij}^{\mathrm{sim}} - Y_{ij}^{\mathrm{exp}}}{\overline{Y_{ij}^{\mathrm{exp}}}}\right|\right) \quad (1)$$

$$E = \frac{1}{N}\sum_{i=1}^{N} E_i \quad (2)$$

$$Y_{ij} = \begin{cases} y_{ij} \\ \ln y_{ij} \end{cases} \quad (3)$$

Here, N is the number of data sets and N_i is the number of data points in the i-th data set. Y_{ij}^{exp} and Y_{ij}^{sim} are the experimental and simulated values of the j-th data point in the i-th data set, respectively. $\overline{Y_{ij}^{\mathrm{exp}}}$ is the average experimental value of the j-th data point in the i-th data set. In eq 3, for the prediction of LBV and SC, $Y_{ij} = y_{ij}$. For the prediction of IDT, $Y_{ij} = \ln y_{ij}$.

For the mechanism evaluation method, Olm et al.[47] selected the error function, $E_i = \frac{1}{N_i}\sum_{j=1}^{N_i}\left(\frac{Y_{ij}^{\mathrm{sim}} - Y_{ij}^{\mathrm{exp}}}{\sigma\left(Y_{ij}^{\mathrm{exp}}\right)}\right)^2$, to evaluate the deviation between the detailed mechanisms and experiments. In this error function, the square root of $(Y_{ij}^{\mathrm{sim}}\text{-}Y_{ij}^{\mathrm{exp}})$ is used. If $(Y_{ij}^{\mathrm{sim}}\text{-}Y_{ij}^{\mathrm{exp}}) > 1$, the error of mechanism will be erroneously exaggerated, and if $(Y_{ij}^{\mathrm{sim}}\text{-}Y_{ij}^{\mathrm{exp}}) < 1$, the error of mechanisms will be erroneously reduced. According to eq 1 recommended by Hu et al.,[30] the absolute value of the difference $(Y_{ij}^{\mathrm{sim}}\text{-}Y_{ij}^{\mathrm{exp}})$ to evaluate the error of mechanisms is used in this work. Compared with previous studies, this mechanism error evaluation method has made significant progress.

2.5. Mechanism Reduction Method. Skeletal mechanisms are obtained by eliminating redundant species and elementary reactions. In this work, systematic reduction for the skeletal mechanism is carried out by using DRGEP and DRGEPSA methods. Then, the obtained skeletal mechanism can maximize the computational speed while ensuring high accuracy.

The direct relationship graph (DRG) method can delete unimportant species within a set error threshold by constructing a directed relationship graph. The error caused by removing species B from the mechanism for the generation of preselected species A is called the correlation coefficient (r_{AB}) between A and B. The DRGEP method considers the error propagation through intermediate species in the reaction pathway from A to B on the basis of DRG. The dependency of species A on species B is represented as

$$r_{\mathrm{AB}} = \frac{|\sum_{i=1}^{n_{\mathrm{R}}} \nu_{\mathrm{A},i}\omega_i\delta_{\mathrm{B}}^i|}{\max(P_{\mathrm{A}}, C_{\mathrm{A}})} \quad (4)$$

where

$$P_{\mathrm{A}} = \sum_{i=1}^{n_{\mathrm{R}}} \max(0, \nu_{\mathrm{A},i}\omega_i) \quad (5)$$

$$C_{\mathrm{A}} = \sum_{i=1}^{n_{\mathrm{R}}} \max(0, -\nu_{\mathrm{A},i}\omega_i) \quad (6)$$

$$\delta_{\mathrm{B}}^i = \begin{cases} 1, & \text{if } i\text{-th elementary reaction involves species B,} \\ 0 & \text{otherwise} \end{cases} \quad (7)$$

https://doi.org/10.1021/acsomega.3c07094
ACS Omega 2023, 8, 47113−47122

Here, $\nu_{A,i}$ is the stoichiometry of species A in the i-th elementary reaction. ω_i is the net reaction rate of the i-th elementary reaction. n_R is the total number of reactions.

The dependency of species A on species B following a certain pathway is represented as

$$r_{AB,p} = \prod_{j=1}^{n-1} r_{s_j s_{j+1}} \tag{8}$$

where s is the intermediate species, e.g., s_1= A, s_n = B, and n is the species numbers in the reaction pathway p. The ultimate dependency of species A on species B is

$$R_{AB} = \max_p(r_{AB,p}) \tag{9}$$

If the dependency of species is lower than the error threshold ε_{EP}, it indicates that the species is redundant, meaning that it has a small impact on the formation and consumption of the target species and needs to be removed from the detailed mechanism under specific conditions. The size of the error threshold ε_{EP} directly affects the accuracy and scale of mechanism. By selection of appropriate ε_{EP}, the skeletal mechanism can be preliminarily obtained.

Then, the DRGEPSA method is further used to reduce the skeletal mechanism. This method requires setting an error threshold e^*, which is usually greater than ε_{EP}. If $R_{AB} > e^*$, the species will be retained, and if $\varepsilon_{EP} < R_{AB} < e^*$, the species will be identified as "limbo" species. Limbo species is first removed to obtain the introduction error, which is represented as

$$\delta_B = |\delta_{B,ind} - \delta_{DRGEP}| \tag{10}$$

where $\delta_{B,ind}$ and δ_{DRGEP} represent the errors introduced after removing species B from the detailed mechanism and skeletal mechanism, respectively. If δ_B is below the user-defined error threshold, species B will be removed and other species will remain in the skeletal mechanism.

2.6. Research Framework. Figure 1 shows the research framework of this work. This work first collects 15 recently developed kinetic models for predicting the cofiring of NH_3/CH_4 and NH_3 combustion and then evaluates the comprehensive performance of the 15 detailed mechanisms based on 1108 experimental data points, obtaining the best detailed mechanism. Then, the detailed mechanism is reduced using DRGEP and DRGEPSA methods for obtaining the skeletal mechanism. Finally, a systematic comparison was made between the skeletal mechanism and the detailed mechanism on predicting LBV, SC, and IDT to verify the accuracy of the skeletal mechanism.

3. RESULTS AND DISCUSSION

3.1. Mechanism Evaluation. *3.1.1. NH_3/CH_4 mechanism evaluation.* Figures 2−4 show the error function values of eight detailed mechanisms for simulating the cofiring of NH_3/CH_4 in predicting LBV, SC, and IDT. It can be seen from the figures that the detailed mechanisms with good accuracy in predicting LBV are the Okafor mechanism, San Diego mechanism, GRI 3.0 mechanism, and Zhou mechanism in order. The detailed mechanism for better measurement accuracy of SC is the Zhou mechanism, and the measurement accuracy of the Glarborg mechanism, Aru mechanism, Dai mechanism, and Okafor mechanism is similar. It is visible in Figure 4 that the Aru mechanism, San Diego mechanism, Tian mechanism, Glarborg mechanism, and Dai mechanism have

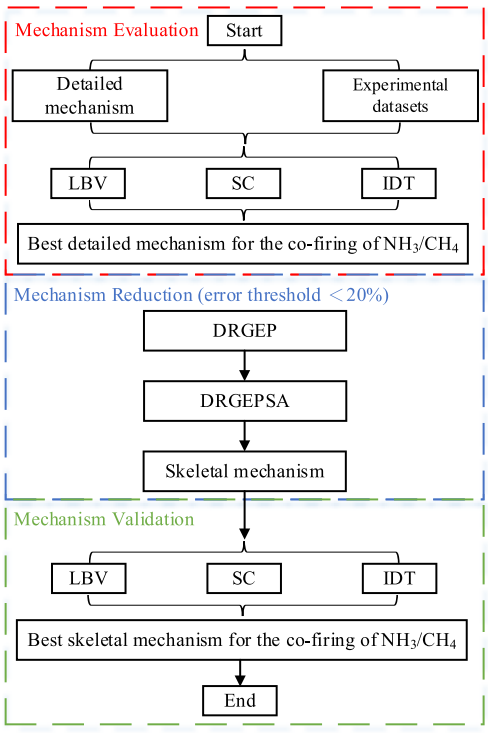

Figure 1. Research framework of this work.

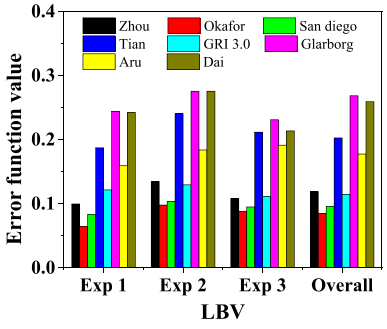

Figure 2. Error function values of eight mechanisms in predicting LBV.

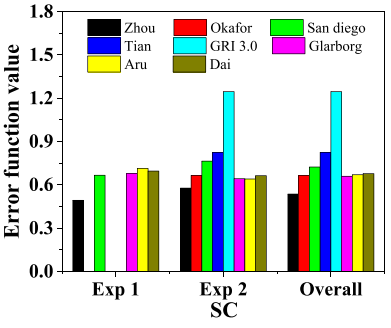

Figure 3. Error function values of eight mechanisms in predicting SC.

high measurement accuracy for IDT. The overall error function values of eight mechanisms in predicting LBV, SC, and IDT are shown in Figure 5. By comprehensively comparing the performance of the eight detailed mechanisms for three combustion parameters, it can be found that the overall error of the Zhou mechanism, Tian mechanism, and Aru mechanism is the smallest. Since the CH_4 chemistry in the

https://doi.org/10.1021/acsomega.3c07094
ACS Omega 2023, 8, 47113−47122

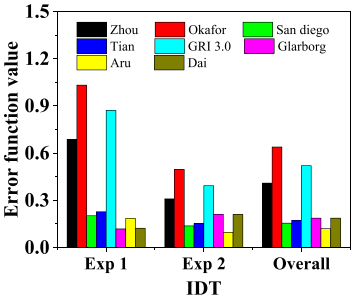

Figure 4. Error function values of eight mechanisms in predicting IDT.

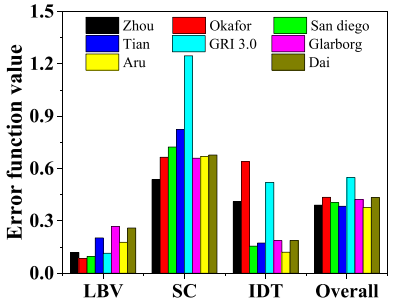

Figure 5. Overall error function values of eight mechanisms in predicting LBV, SC, and IDT.

mechanisms has been validated during the past decades, we will evaluate the ammonia chemistry of these mechanisms.

3.1.2. NH_3 Mechanism Evaluation. Figures 6−9 show the overall error function values of 10 detailed mechanism for

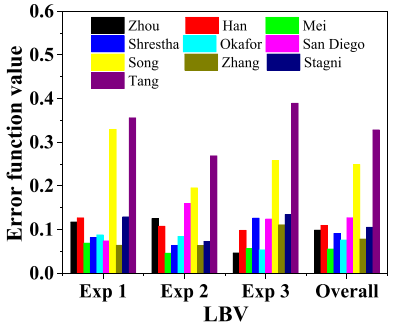

Figure 6. Error function values of 10 mechanisms in predicting LBV.

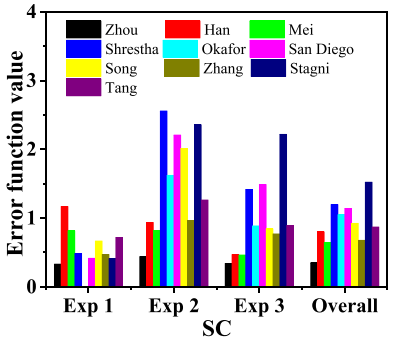

Figure 7. Error function values of 10 mechanisms in predicting SC.

simulating NH_3 combustion in predicting LBV, SC, and IDT. Due to the large deviation of GRI 3.0, Glarborg, and Dai mechanisms in predicting the cofiring of NH_3/CH_4, the large

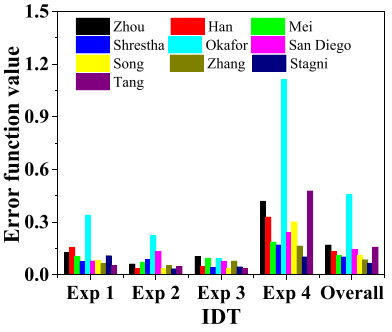

Figure 8. Error function values of 10 mechanisms in predicting IDT.

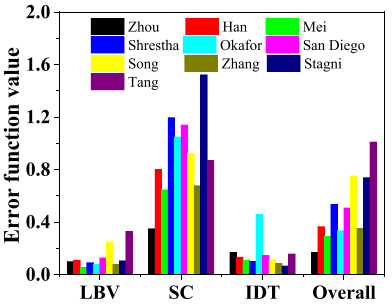

Figure 9. Overall error function values of 10 mechanisms in predicting LBV, SC, and IDT.

deviation of the Tian mechanism in predicting the ammonia chemistry, and ammonia chemistry in the Aru mechanism being the same as that in the Stagni mechanism, the evaluation of ammonia chemistry on the five mechanisms will not be further presented in the following.

It can be seen from the figures that the detailed mechanisms with good accuracy in predicting LBV are the Mei mechanism, Okafor mechanism, and Zhang mechanism in order. The Zhou mechanism has significant advantages in predicting SC of ammonia oxidation followed by Zhang and Mei mechanisms. The smallest deviation in predicting IDT of NH_3 is found by the Stagni mechanism followed by Zhang and Shrestha mechanisms. As shown in Figure 9, the Zhou mechanism has achieved the best performance, especially in SC, which is mainly attributed to the updates in N_2O chemistry and NH_2 chemistry.[23] Additionally, the main advantage of the Tian mechanism and Aru mechanism lies in the prediction of IDT, while the main advantage of the Zhou mechanism lies in the prediction of SC. It should be mentioned that the prediction accuracy of the Zhou model for ammonia combustion is significantly better than that of the Aru model, but the overall simulation error of the two models for NH_3/CH_4 combustion is almost the same and small. Although the Aru model and Zhou model have similar CH_4 chemistry, the NH_3 chemistry and C−N interaction mechanism are totally different. The C−N interaction mechanism will significantly affect the production of key species such as NO and N_2O and has a key impact on the prediction of SC.[23] Therefore, a comprehensive comparison between the Aru model and Zhou model has been performed, and the Zhou model is selected for mechanism reduction.

3.2. Mechanism Reduction. The Zhou mechanism includes 169 species and 1268 elementary reactions. DRGEP and DRGEPSA methods are used for mechanism reduction in

https://doi.org/10.1021/acsomega.3c07094
ACS Omega 2023, 8, 47113−47122

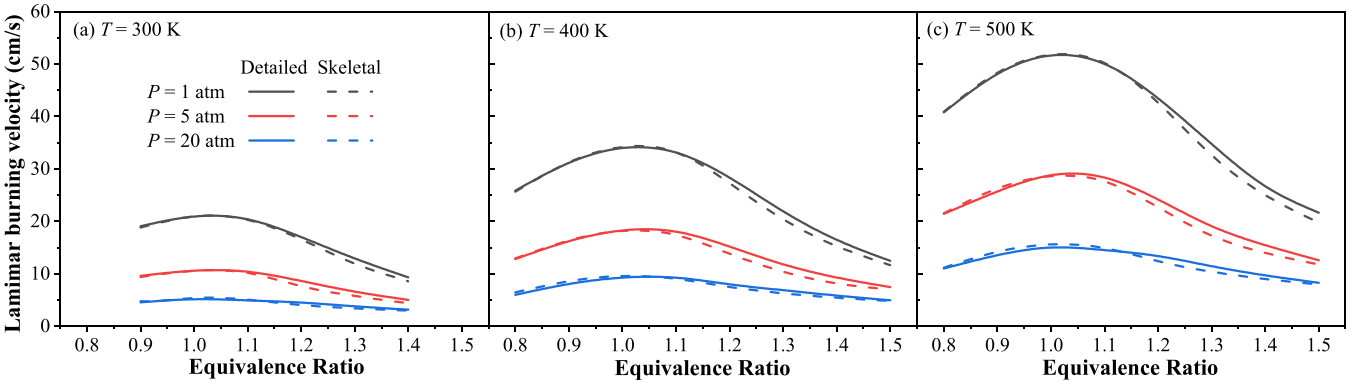

Figure 10. (a−c) Validation of the laminar burning velocity predicted by the detailed mechanism and skeletal mechanism.

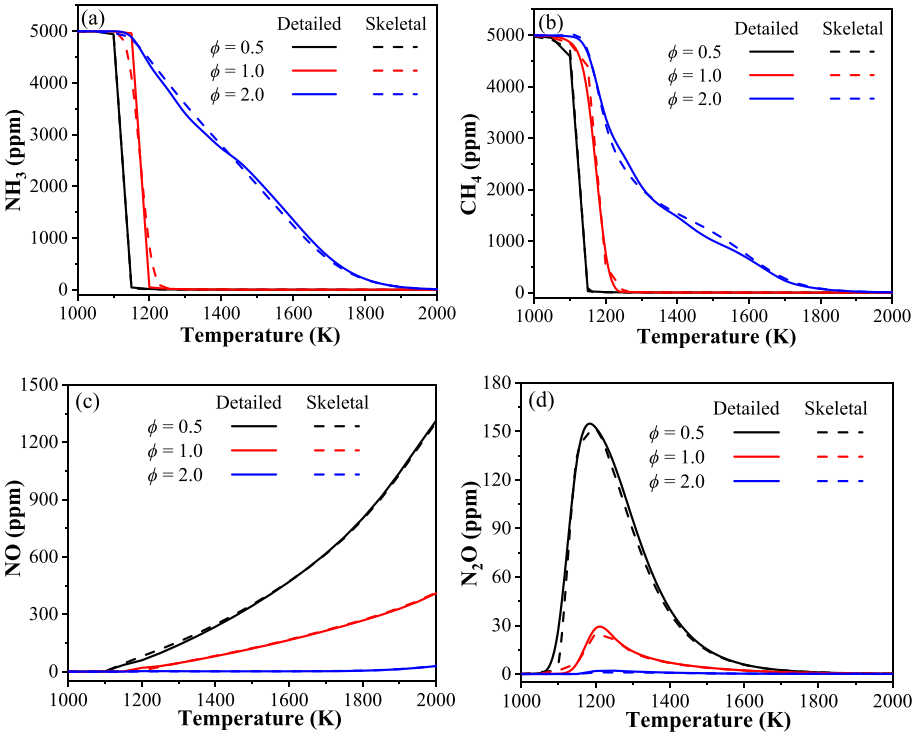

Figure 11. Validation of (a) NH_3, (b) CH_4, (c) NO, and (d) N_2O predicted by the detailed mechanism and skeletal mechanism in PSR.

this work. Redundant species and reactions are deleted to obtain the simplest skeletal mechanism.

In the DRGEP method, CH_4, CO_2, NH_3, O_2, N_2, H_2O, HCN, NO, and OH are selected as the target species, and ε_{EP} is determined to be 0.2. In the working conditions, the temperature covers 1000−2000 K, the equivalence ratio covers 0.5−2.0, the pressure covers 1−60 atm, and the mole fractions of NH_3/CH_4 are 50%/50%. A preliminary skeletal mechanism of 55 species and 437 elementary reactions is obtained by the DRGEP method.

In the DRGEPSA method, e^* is also determined as 0.2. Then, 10 species and 93 elementary reactions are deleted and an optimal skeletal mechanism of 45 species and 344 elementary reactions is developed. By systematically simplifying the mechanism, the skeletal mechanism obtained in this work can achieve a computational acceleration of $(169/45)^2 = 14.1$.[30] The skeletal mechanism is shown in the Supporting Information.

The skeletal mechanism obtained in this work can significantly reduce computational costs without reducing accuracy compared with the original mechanism and can be coupled with a finite rate combustion model in CFD software to achieve simulation of the combustion process. The skeletal mechanism mainly focuses on the formation of various nitrogen-containing pollutants for the cofiring of NH_3/CH_4, e.g., NO, N_2O, and HCN. It can also be applied to the combustion simulation of fuels (coal, biomass, etc.) using HCN and NH_3 as nitrogen sources.

3.3. Mechanism Validation. The skeletal mechanism and detailed mechanism are compared in detail, including the laminar flame velocity using the module of premixed laminar flame speed, the main oxidation products using the module of perfect stirred reactor and plug flow reactor, and the ignition delay time using the module of homogeneous.

3.3.1. Laminar Burning Velocity. Figure 10 shows the validation of laminar burning velocity predicted by the detailed mechanism and skeletal mechanism. In the verification of laminar flame velocity, the equivalence ratio covers 0.8−1.5, the initial temperatures are 300−500 K, and the initial pressures are 1, 5, and 20 atm, respectively. Although the

https://doi.org/10.1021/acsomega.3c07094
ACS Omega 2023, 8, 47113−47122

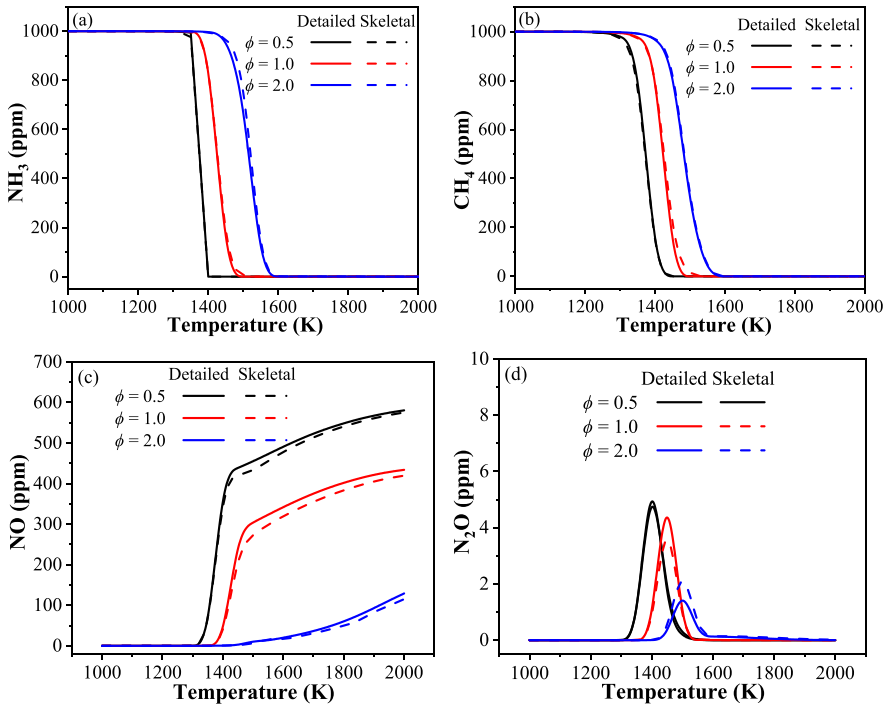

Figure 12. Validation of (a) NH_3, (b) CH_4, (c) NO, and (d) N_2O predicted by the detailed mechanism and skeletal mechanism in PFR.

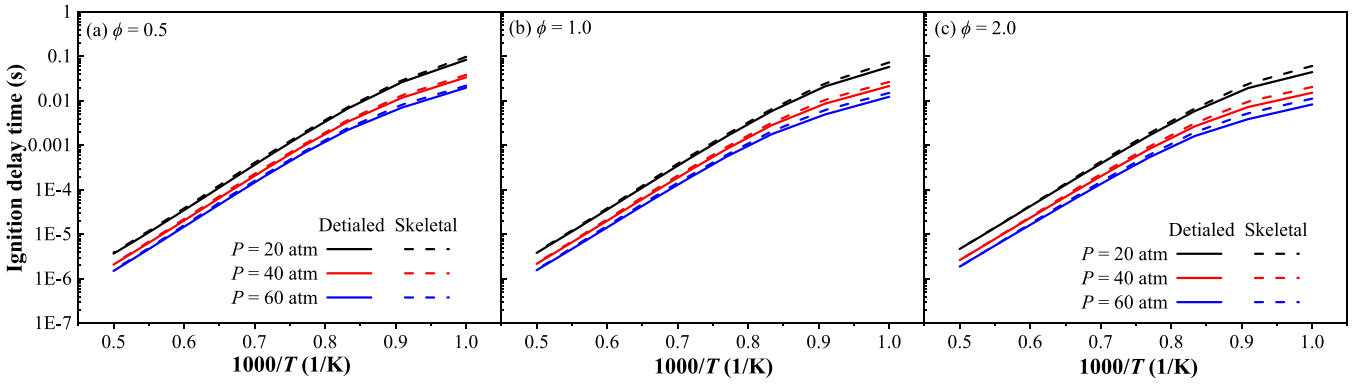

Figure 13. (a−c) Validation of the ignition delay time predicted by the detailed mechanism and skeletal mechanism.

maximum pressure was set to 60 atm during the process of simplifying the detailed mechanism, it can be found that as the pressure increased, the laminar flame velocity gradually decreased and the laminar flame velocity was too slow to calculate due to excessive pressure in verifying the skeletal mechanism. Therefore, the maximum pressure was set at 20 atm. The experimental gas composition is NH_3/CH_4/air, and the mole fractions of NH_3/CH_4 are 50%/50%. As is shown in the picture, the prediction of laminar flame velocity between the skeletal mechanism and the detailed mechanism has very little difference in the fuel-lean conditions, and there is a small amount of error in the fuel-rich conditions. The maximum absolute error is less than 2 cm/s, and the maximum relative error is less than 10%. It indicates that there is good consistency between the skeletal mechanism and the detailed mechanism in the prediction of laminar flame velocity.

3.3.2. Species Concentration. Figure 11 shows the validation of species concentration predicted by the detailed mechanism and skeletal mechanism in PSR. In the verification of species concentration, the equivalence ratio covers 0.5−2.0, the oxidation temperature covers 1000−2000 K, the pressure is 1 atm, the mole fractions of NH_3/CH_4 are all 5000 ppm, the residence time is 1.5 s, and the diluent is argon (Ar). Finally, the concentration changes of NH_3, CH_4, NO, and N_2O predicted by the skeletal mechanism and detailed mechanisms are obtained. As illustrated in the figure, regardless of the changes in the equivalence ratio and oxidation temperature, the skeletal mechanism can effectively predict the concentration changes of NH_3, CH_4, NO, and N_2O. The maximum deviation between the skeletal mechanism and detailed mechanism in NH_3/CH_4 reactivity does not exceed 25 K. Additionally, there is good consistency in the formation of NO and N_2O between the skeletal mechanism and detailed mechanism.

Figure 12 shows the validation of species concentration predicted by the detailed mechanism and skeletal mechanism in PFR. In the verification of species concentration, the equivalence ratio covers 0.5−2.0, the oxidation temperature covers 1000−2000 K, the pressure is 1.25 atm, the constant temperature zone length of the reaction zone is set to 100 cm, the reactor diameter is 4 mm, the diluent is helium (He), the total volume flow rate is 1.51×10^{-4} m^3/s, and the mole

https://doi.org/10.1021/acsomega.3c07094
ACS Omega 2023, 8, 47113−47122

fractions of NH_3 and CH_4 are 50%/50%, both of which are 1000 ppm. It can be seen from the figure that the skeletal mechanism and detailed mechanism have good consistency in predicting the change tendency of NH_3, CH_4, NO, and N_2O. The maximum deviation between the skeletal mechanism and detailed mechanism for NO prediction is less than 6.5%.

Figure 13 shows the validation of ignition delay time predicted by the detailed mechanism and skeletal mechanism in homogeneous. The equivalence ratio covers 0.5−2.0, the oxidation temperature covers 1000−2000 K, the pressure covers 20−60 atm, and the mole fractions of NH_3 and CH_4 are both 50%. As shown in the picture, the predicted results of the skeletal mechanism are in good agreement with the predicted results of the detailed mechanism under both fuel-lean and fuel-rich conditions. The main deviation between the skeletal mechanism and the detailed mechanism occurs under low-temperature and fuel-rich conditions, but the maximum deviation is less than 13%.

4. CONCLUSIONS

This work comprehensively evaluated the predictive performance of the 15 mechanisms on laminar burning velocity (LBV), species concentration (SC), and ignition delay time (IDT), obtained the optimal detailed mechanism, and carried out mechanism reduction and verification. The main conclusions of this work are as follows:

(1) Based on 19 experimental data sets with a total of 1108 data points and 15 detailed mechanisms for the cofiring of NH_3/CH_4 and NH_3 combustion, it is found that the Zhou mechanism has the best performance in predicting laminar flame velocity, species concentration, and ignition delay time of NH_3/CH_4 cofiring and NH_3 combustion.

(2) Using the Zhou mechanism as the target mechanism and DRGEP and DRGEPSA as the mechanism reduction methods, the skeletal mechanism of 45 species and 344 elementary reactions is obtained. Compared with the detailed mechanism, the skeletal mechanism can achieve 14.1 times faster computational acceleration.

(3) Detailed and skeletal mechanisms are used to simulate LBV, SC, and IDT, covering the temperatures of 1000−2000 K, pressures of 1−60 atm, and equivalence ratios of 0.5−2.0. The maximum error between the skeletal mechanism and the detailed mechanism is less than 13%.

■ ASSOCIATED CONTENT

Supporting Information

The Supporting Information is available free of charge at https://pubs.acs.org/doi/10.1021/acsomega.3c07094.

Skeletal mechanism (TXT)

■ AUTHOR INFORMATION

Corresponding Author

Houzhang Tan − *MOE Key Laboratory of Thermo-Fluid Science and Engineering, Department of Thermal Engineering, Xi'an Jiaotong University, Xi'an, Shaanxi Province 710049, China;* orcid.org/0000-0002-8723-1949; Email: hzt@mail.xjtu.edu.cn

Authors

Yuhang Li − *State Key Laboratory of Multiphase Flow in Power Engineering, Department of Thermal Engineering, Xi'an Jiaotong University, Xi'an, Shaanxi Province 710049, China*

Zhonghua Jin − *Xi'an Thermal Power Research Institute Co., Ltd., Xi'an, Shaanxi Province 710054, China*

Zhichao Wang − *Xi'an Thermal Power Research Institute Co., Ltd., Xi'an, Shaanxi Province 710054, China*

Zixiu Jia − *Xi'an Thermal Power Research Institute Co., Ltd., Xi'an, Shaanxi Province 710054, China*

Baochong Cui − *MOE Key Laboratory of Thermo-Fluid Science and Engineering, Department of Thermal Engineering, Xi'an Jiaotong University, Xi'an, Shaanxi Province 710049, China*

Shangkun Zhou − *MOE Key Laboratory of Thermo-Fluid Science and Engineering, Department of Thermal Engineering, Xi'an Jiaotong University, Xi'an, Shaanxi Province 710049, China*

Faqi Bai − *Huaneng Power International, Inc., Beijing 100084, China*

Complete contact information is available at: https://pubs.acs.org/10.1021/acsomega.3c07094

Notes

The authors declare no competing financial interest.

■ ACKNOWLEDGMENTS

This work was supported by the Science and Technology Project of Huaneng Power International (HNK21-HF304): High-efficiency and Low-nitrogen Combustion Technology Development of the Combustion of Ammonia with Natural Gas and Coal.

■ REFERENCES

(1) MacFarlane, D. R.; Cherepanov, P. V.; Choi, J.; Suryanto, B. H. R.; Hodgetts, R. Y.; Bakker, J. M.; Ferrero Vallana, F. M.; Simonov, A. N. A Roadmap to the Ammonia Economy. *Joule* **2020**, *4* (6), 1186−1205.

(2) Valera-Medina, A.; Xiao, H.; Owen-Jones, M.; David, W. I. F.; Bowen, P. J. Ammonia for power. *Prog. Energy Combust. Sci.* **2018**, *69*, 63−102.

(3) Valera-Medina, A.; Amer-Hatem, F.; Azad, A. K.; Dedoussi, I. C.; de Joannon, M.; Fernandes, R. X.; Glarborg, P.; Hashemi, H.; He, X.; Mashruk, S.; et al. Review on Ammonia as a Potential Fuel: From Synthesis to Economics. *Energy Fuels* **2021**, *35* (9), 6964−7029.

(4) Kobayashi, H.; Hayakawa, A.; Somarathne, K. D. K. A.; Okafor, E. C. Science and technology of ammonia combustion. *Proc. Combust. Inst.* **2019**, *37* (1), 109−133.

(5) Stagni, A.; Cavallotti, C.; Arunthanayothin, S.; Song, Y.; Herbinet, O.; Battin-Leclerc, F.; Faravelli, T. An experimental, theoretical and kinetic-modeling study of the gas-phase oxidation of ammonia. *Reaction Chemistry & Engineering* **2020**, *5* (4), 696−711.

(6) Sorrentino, G.; Sabia, P.; Bozza, P.; Ragucci, R.; de Joannon, M. Low-NOx conversion of pure ammonia in a cyclonic burner under locally diluted and preheated conditions. *Appl. Energy* **2019**, *254*, No. 113676.

(7) Ariemma, G. B.; Sabia, P.; Sorrentino, G.; Bozza, P.; de Joannon, M.; Ragucci, R. Influence of water addition on MILD ammonia combustion performances and emissions. *Proc. Combust. Inst.* **2021**. DOI: 385147.

(8) Han, X.; Wang, Z.; Costa, M.; Sun, Z.; He, Y.; Cen, K. Experimental and kinetic modeling study of laminar burning velocities of NH_3/air, NH_3/H_2/air, NH_3/CO/air and NH_3/CH_4/air premixed flames. *Combust. Flame* **2019**, *206*, 214−226.

(9) Ariemma, G. B.; Sorrentino, G.; Ragucci, R.; de Joannon, M.; Sabia, P. Ammonia/Methane combustion: Stability and NOx emissions. *Combust. Flame* **2022**, *241*, No. 112071.

(10) Shrestha, K. P.; Lhuillier, C.; Barbosa, A. A.; Brequigny, P.; Contino, F.; Mounaïm-Rousselle, C.; Seidel, L.; Mauss, F. An experimental and modeling study of ammonia with enriched oxygen content and ammonia/hydrogen laminar flame speed at elevated pressure and temperature. *Proc. Combust. Inst.* **2021**, *38* (2), 2163−2174.
(11) Zhou, S.; Yang, W.; Tan, H.; An, Q.; Wang, J.; Dai, H.; Wang, X.; Wang, X.; Deng, S. Experimental and kinetic modeling study on NH_3/syngas/air and NH_3/bio-syngas/air premixed laminar flames at elevated temperature. *Combust. Flame* **2021**, *233*, No. 111594.
(12) Mei, B.; Ma, S.; Zhang, Y.; Zhang, X.; Li, W.; Li, Y. Exploration on laminar flame propagation of ammonia and syngas mixtures up to 10 atm. *Combust. Flame* **2020**, *220*, 368−377.
(13) Wei, F.; Wang, P.; Cao, J.; Long, W.; Dong, D.; Tian, H.; Tian, J.; Zhang, X.; Lu, M. Visualization investigation of jet ignition ammonia-methanol by an ignition chamber fueled H2. *Fuel* **2023**, *349*. DOI: 128658.
(14) Lu, M.; Dong, D.; Wei, F.; Long, W.; Wang, Y.; Cong, L.; Dong, P.; Tian, H.; Wang, P. Chemical mechanism of ammonia-methanol combustion and chemical reaction kinetics analysis for different methanol blends. *Fuel* **2023**, *341*. DOI: 127697.
(15) Jin, S.; Tu, Y.; Liu, H. Experimental study and kinetic modeling of NH3/CH4 co-oxidation in a jet-stirred reactor. *Int. J. Hydrogen Energy* **2022**, *47* (85), 36323−36341.
(16) Zhang, J.; Ito, T.; Ishii, H.; Ishihara, S.; Fujimori, T. Numerical investigation on ammonia co-firing in a pulverized coal combustion facility: Effect of ammonia co-firing ratio. *Fuel* **2020**, *267*, No. 117166.
(17) Tamura, M.; Gotou, T.; Ishii, H.; Riechelmann, D. Experimental investigation of ammonia combustion in a bench scale 1.2 MW-thermal pulverised coal firing furnace. *Appl. Energy* **2020**, *277*, No. 115580.
(18) Okafor, E. C.; Naito, Y.; Colson, S.; Ichikawa, A.; Kudo, T.; Hayakawa, A.; Kobayashi, H. Experimental and numerical study of the laminar burning velocity of CH_4-NH_3-air premixed flames. *Combust. Flame* **2018**, *187*, 185−198.
(19) Glarborg, P.; Miller, J. A.; Ruscic, B.; Klippenstein, S. J. Modeling nitrogen chemistry in combustion. *Prog. Energy Combust. Sci.* **2018**, *67*, 31−68.
(20) Dai, L.; Gersen, S.; Glarborg, P.; Mokhov, A.; Levinsky, H. Autoignition studies of NH_3/CH_4 mixtures at high pressure. *Combust. Flame* **2020**, *218*, 19−26.
(21) Arunthanayothin, S.; Stagni, A.; Song, Y.; Herbinet, O.; Faravelli, T.; Battin-Leclerc, F. Ammonia-methane interaction in jet-stirred and flow reactors: An experimental and kinetic modeling study. *Proc. Combust. Inst.* **2021**, *38* (1), 345−353.
(22) Zhou, S.; Cui, B.; Yang, W.; Tan, H.; Wang, J.; Dai, H.; Li, L.; Rahman, Z. u.; Wang, X.; Deng, S.; et al. An experimental and kinetic modeling study on NH_3/air, NH_3/H_2/air, NH_3/CO/air, and NH_3/CH_4/air premixed laminar flames at elevated temperature. *Combust. Flame* **2023**, *248*, No. 112536.
(23) Zhou, S.; Yang, W.; Zheng, S.; Yu, S.; Tan, H.; Cui, B.; Wang, J.; Deng, S.; Wang, X. An experimental and kinetic modeling study on the low and intermediate temperatures oxidation of NH_3/O_2/Ar, NH_3/H_2/O_2/Ar, NH_3/CO/O_2/Ar, and NH_3/CH_4/O_2/Ar mixtures in a jet-stirred reactor. *Combust. Flame* **2023**, *248*, No. 112529.
(24) Lu, T.; Law, C. K. A directed relation graph method for mechanism reduction. *Proceedings of the Combustion Institute* **2005**, *30* (1), 1333−1341.
(25) Pepiot-Desjardins, P.; Pitsch, H. An efficient error-propagation-based reduction method for large chemical kinetic mechanisms. *Combust. Flame* **2008**, *154* (1−2), 67−81.
(26) Borger, I.; Merkel, A.; Lachmann, J.; Spangenberg, H. J.; Turanyi, T. An extended kinetic model and its reduction by sensitivity analysis for the methanol/oxygen gas-phase thermolysis. *ACH - Models Chem.* **1992**, *129*, 855−864.
(27) Lam, S. H. Using CSP to understand complex chemical kinetics. *Combust. Sci. Technol.* **1993**, *89* (5−6), 375−404.
(28) Zhang, X.; Sarathy, S. M. A functional-group-based approach to modeling real-fuel combustion chemistry − II: Kinetic model construction and validation. *Combust. Flame* **2021**, *227*, 510−525.
(29) Li, W.; Xuan, T.; Wang, Q.; Dai, L. A novel object-oriented directed path screening method for reduction of detailed chemical kinetic mechanism. *Combust. Flame* **2023**, *251*, No. 112727.
(30) Hu, F.; Li, P.; Wang, K.; Li, W.; Guo, J.; Liu, L.; Liu, Z. Evaluation, development, and application of a new skeletal mechanism for fuel-NO formation under air and oxy-fuel combustion. *Fuel Process. Technol.* **2020**, *199*, No. 106256.
(31) *GRI Mech 3.0. Gas Research Institute*, available at < http://www.me.berkeley.edu/gri _mech/>. (accessed.
(32) Tian, Z.; Li, Y.; Zhang, L.; Glarborg, P.; Qi, F. An experimental and kinetic modeling study of premixed NH_3/CH_4/O_2/Ar flames at low pressure. *Combust. Flame* **2009**, *156* (7), 1413−1426.
(33) Chemical-kinetic mechanisms for combustion applications, mechanical and aerospace engineering (combustion research). University of California at San Diego. (accessed.
(34) Zhou, C.-W.; Li, Y.; Burke, U.; Banyon, C.; Somers, K. P.; Ding, S.; Khan, S.; Hargis, J. W.; Sikes, T.; Mathieu, O.; et al. An experimental and chemical kinetic modeling study of 1,3-butadiene combustion: Ignition delay time and laminar flame speed measurements. *Combust. Flame* **2018**, *197*, 423−438.
(35) Song, Y.; Hashemi, H.; Christensen, J. M.; Zou, C.; Marshall, P.; Glarborg, P. Ammonia oxidation at high pressure and intermediate temperatures. *Fuel* **2016**, *181*, 358−365.
(36) Han, X.; Wang, Z.; He, Y.; Zhu, Y.; Cen, K. Experimental and kinetic modeling study of laminar burning velocities of NH_3/syngas/air premixed flames. *Combust. Flame* **2020**, *213*, 1−13.
(37) Shrestha, K. P.; Lhuillier, C.; Barbosa, A. A.; Brequigny, P.; Contino, F.; Mounaïm-Rousselle, C.; Seidel, L.; Mauss, F. An experimental and modeling study of ammonia with enriched oxygen content and ammonia/hydrogen laminar flame speed at elevated pressure and temperature. *Proceedings of the Combustion Institute* **2021**, *38* (2), 2163−2174.
(38) Zhang, X.; Moosakutty, S. P.; Rajan, R. P.; Younes, M.; Sarathy, S. M. Combustion chemistry of ammonia/hydrogen mixtures: Jet-stirred reactor measurements and comprehensive kinetic modeling. *Combust. Flame* **2021**, *234*. DOI: 111653.
(39) Tang, R.; Xu, Q.; Pan, J.; Gao, J.; Wang, Z.; Wei, H.; Shu, G. An experimental and modeling study of ammonia oxidation in a jet stirred reactor. *Combust. Flame* **2022**, *240*. DOI: 112007.
(40) Okafor, E. C.; Naito, Y.; Colson, S.; Ichikawa, A.; Kudo, T.; Hayakawa, A.; Kobayashi, H. Measurement and modelling of the laminar burning velocity of methane-ammonia-air flames at high pressures using a reduced reaction mechanism. *Combust. Flame* **2019**, *204*, 162−175.
(41) Shu, T.; Xue, Y.; Zhou, Z.; Ren, Z. An experimental study of laminar ammonia/methane/air premixed flames using expanding spherical flames. *Fuel* **2021**, *290*, No. 120003.
(42) Mei, B.; Zhang, X.; Ma, S.; Cui, M.; Guo, H.; Cao, Z.; Li, Y. Experimental and kinetic modeling investigation on the laminar flame propagation of ammonia under oxygen enrichment and elevated pressure conditions. *Combust. Flame* **2019**, *210*, 236−246.
(43) Shu, B.; Vallabhuni, S. K.; He, X.; Issayev, G.; Moshammer, K.; Farooq, A.; Fernandes, R. X. A shock tube and modeling study on the autoignition properties of ammonia at intermediate temperatures. *Proceedings of the Combustion Institute* **2019**, *37* (1), 205−211.
(44) Mathieu, O.; Kopp, M. M.; Petersen, E. L. Shock-tube study of the ignition of multi-component syngas mixtures with and without ammonia impurities. *Proceedings of the Combustion Institute* **2013**, *34* (2), 3211−3218.
(45) Chen, J.; Jiang, X.; Qin, X.; Huang, Z. Effect of hydrogen blending on the high temperature auto-ignition of ammonia at elevated pressure. *Fuel* **2021**, *287*. DOI: 119563.
(46) Dai, L.; Gersen, S.; Glarborg, P.; Levinsky, H.; Mokhov, A. Experimental and numerical analysis of the autoignition behavior of NH3 and NH3/H2 mixtures at high pressure. *Combust. Flame* **2020**, *215*, 134−144.

https://doi.org/10.1021/acsomega.3c07094
ACS Omega 2023, 8, 47113−47122

(47) Olm, C.; Zsély, I. G.; Varga, T.; Curran, H. J.; Turányi, T. Comparison of the performance of several recent syngas combustion mechanisms. *Combust. Flame* **2015**, *162* (5), 1793−1812.

https://doi.org/10.1021/acsomega.3c07094
ACS Omega 2023, 8, 47113−47122